Catalytic Degradation of Polystyrene: Modeling of Molecular Weight Distribution

Ioana A. Gianoglio Pantano, Mariano Asteasuain, Mónica F. Díaz, Claudia Sarmoria, Adriana Brandolin*

Two of the most abundant polymers in household waste streams, PS and PE, may be recycled by compatibilization through a Friedel-Crafts alkylation. This reaction produces a graft copolymer PE-*g*-PS that improves the properties of the blend, but simultaneously degrades PS chains. Since the copolymer efficiency as a compatibilizer depends both on the molecular weight and MWD of its two blocks, the operating conditions for the copolymer synthesis must be carefully tuned. To aid in this task, we present a preliminary mathematical model that focuses on the effect of the catalyst and cocatalyst of the Friedel-Crafts alkylation on the MWD of the PS chains. The model's predictions are shown to agree with experimental data.

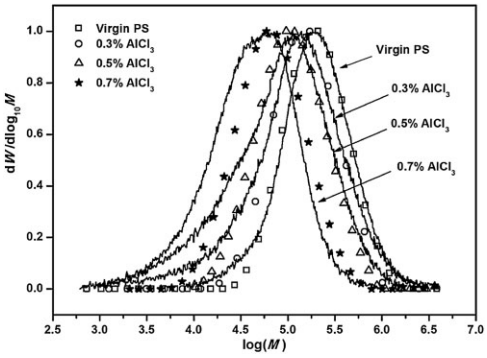

Introduction

The recycling of thermoplastic polymers is an attractive approach to the reduction of plastic waste accumulation. However, since most waste streams contain several different immiscible thermoplastics, the task requires implementing either separation protocols or compatibilization methods. The latter strategy may be achieved in several ways, one of which is the reactive processing of the mixed polymers in conditions that promote the synthesis of a graft copolymer that could act as a compatibilizer. Since polystyrene (PS) and the polyolefins (PO) are two of the majority components in household plastic waste streams, there is an interest in developing strategies for dealing with mixtures of these two types of resins. Several authors have reported the use of Friedel-Crafts alkylations to achieve the reactive compatibilization of mixtures of PS and PO.[1–6] The reported alkylation reaction, catalyzed by aluminum chloride ($AlCl_3$) and styrene (S), produces a graft copolymer that improves the properties of the blend.[1,3,4] The appropriateness of the copolymer as a compatibilizer depends strongly on the molecular weight and molecular weight distribution (MWD) of its two blocks. Experimental evidence indicates that under typical processing conditions PE is practically unchanged. Unfortunately, the same reaction conditions that promote the synthesis of the graft copolymer also lead to PS degradation.[7–10] Balancing the two types of reaction requires careful tuning of the reaction conditions, a task for which a mathematical model could prove very useful.

In a preliminary model published previously, we considered PS degradation in the presence of $AlCl_3$ only.[11] That model was able to predict the evolution of PS average molecular weights during the reaction. In a second model we considered the effect of processing PE and PS in the presence of both $AlCl_3$ and S. Here, the PE/PS grafting reaction competed with degradation reactions.[12] In this case, we were able to accurately predict the mass of grafted PS, as well as the average molecular weights of PS during the reaction. However, since the final properties of the treated mixture depend not only on average molecular weights but also on the complete MWD, it would be extremely useful to add the capability of predicting MWD to our previous grafting model.

In this work, as a first step in the construction of a complete mathematical model of the graft reaction, we

I. A. Gianoglio Pantano, M. Asteasuain, M. F. Díaz, C. Sarmoria, A. Brandolin
Planta Piloto de Ingeniería Química, PLAPIQUI (UNS-CONICET), Camino La Carrindanga km 7, 8000 Bahía Blanca, Argentina
E-mail: abrandolin@plapiqui.edu.ar

DOI: 10.1002/mren.201100001

have studied the degradation of PS in the presence of a catalyst ($AlCl_3$) and a cocatalyst (S) appropriate for a Friedel-Crafts reaction. The objective is to be able to predict the MWD of the degraded PS. We use the complete kinetic mechanism proposed by Gianoglio Pantano et al.[12] except for the steps describing PE grafting. In order to achieve the MWD prediction we apply a transform technique to the mass balances derived from the proposed kinetic mechanism. The chosen transform is the probability-generating function (pgf). This transformation results in pgf balances for the MWD expressed in number fraction distribution (MWDn), weight fraction distribution (MWDw), or differential-log distribution ($dW/d\log_{10} M$). Initial pgf values are calculated from the initial MWD of the PS obtained from size-exclusion chromatography (SEC) measurements. In order to obtain the MWD of the modified polymer, the pgfs calculated from the balances are inverted numerically using the method reported in Asteasuain et al.[13] for the inversion of the pgf of polymeric systems.

Mathematical Model

Our previous model of the graft copolymerization of PS and PE[12] included the degradation of PS in the presence of $AlCl_3$. In that work we used the well-known method of moments to calculate the PS average molecular weights. Here we use the same kinetic mechanism, in which we consider that the reaction of PS with $AlCl_3$ alone or with the system $AlCl_3$/S leads initially to the elimination of a PS phenyl group, generating a benzene molecule and a polymeric carbonium ion. Afterward, the carbonium ion may induce chain scission in PS. This scission is assumed to be produced by the cleavage of two types of PS links: "weak" and "normal." Chain combination is also considered, as well as the formation of indane structures in the backbone. Besides taking part of scission and combination reactions, S may also polymerize. Finally, the proposed mechanism takes into account the deactivation of the catalytic system. All these steps are summarized in Table 1, together with the corresponding reaction rates. The latter are indicated as R_i,

Table 1. Kinetic model.

Kinetic equation	R_i
chain scission through weak links (I):	$R_1(x) = k_{S1w} f_w A^2 x\,PS(x)$
$PS(x) + A \xrightarrow{k_{S1w}} PS(x-y-1) + PS(y) + A + B, \quad x = 2,\ldots,\infty$ (1)	
chain scission through weak links (II):	$R_2(x) = k_{S2w} f_w A^2 S^2 x\,PS(x)$
$PS(x) + A + S \xrightarrow{k_{S2w}} PS(x-y-1) + PS(y) + A + B + S, \quad x = 2,\ldots,\infty$ (2)	
chain scission through normal links (I):	$R_3(x) = k_{S1n} f_n A^4 x\,PS(x)$
$PS(x) + A \xrightarrow{k_{S1n}} PS(x-y-1) + PS(y) + A + B, \quad x = 2,\ldots,\infty$ (3)	
chain scission through normal links (II):	$R_4(x) = k_{S2n} f_n A^4 S^1 x\,PS(x)$
$PS(x) + A + S \xrightarrow{k_{S2n}} PS(x-y-1) + PS(y) + A + B + S, \quad x = 2,\ldots,\infty$ (4)	
formation of indane skeleton:	$R_5(x) = k_{In} A^2 x\,PS(x)$
$PS(x) + A \xrightarrow{k_{In}} PS(x-1) + A + B, \quad x = 2,\ldots,\infty$ (5)	
chain combination (I):	$R_6(x,y) = k_{c1} A^2 x\,PS(x)\,y\,PS(y)$
$PS(x) + PS(y) + A \xrightarrow{k_{c1}} PS(x+y) + A, \quad x = 2,\ldots,\infty$ (6)	
chain combination (II):	$R_7(x,y) = \left(k_{c2,1} A^2 S^1 + k_{c2,2} A^4 S^4\right) x\,PS(x)\,y\,PS(y)$
$PS(x) + PS(y) + A + S \xrightarrow{k_{c2}} PS(x+y) + A + S, \quad x = 2,\ldots,\infty$ (7)	
styrene polymerization:	$R_8(x) = 2k_p A^2 S^2 PS(x)$
$PS(x) + A + S \xrightarrow{k_p} PS(x+1) + A, \quad x = 1,\ldots,\infty$ (8)	
catalytic system deactivation:	
catalyst decomposition:	$R_9 = k_i A$
$A \xrightarrow{k_i} A_i$ (9)	
catalyst-styrene reaction:	$R_{10} = k_d A^2 S^3$
$A + S \xrightarrow{k_d} A_i + S_i$ (10)	

where i is the equation number. Additional details about the kinetic mechanism can be found in our previous work.[12]

In Equation 1–10, shown in Table 1, PS(x) is a PS molecule with x monomeric units, S is a styrene molecule, A is an active catalyst molecule, A_i and S_i are the inactive catalyst and cocatalyst molecules, and B is a benzene molecule.

We assume that PS(x) has x reactive sites for every reaction except the one shown in Equation 8, where it may only react through two sites. All reactions are first-order with respect to the reactive sites. The reaction orders with respect to the catalyst and cocatalyst concentrations together with the kinetic rate constants were estimated in a previous work.[12]

The process is considered to be carried out in a constant volume, stirred batch reactor at isothermal conditions. The mass balances for the species that take part of the reactions described in Equation 1–10 are presented in Equation 11–14. In what follows, we omit the use of brackets to indicate the molar concentration of each species.

Mass Balances

PS Molecules with x Monomeric Units ($x = 1, \ldots, \infty$):

$$\begin{aligned}\frac{dPS(x)}{dt} =& -\sum_{i=1}^{4} R_i(x)\left(1-\delta_{x,1}\right) + 2\sum_{y=x+1}^{\infty} \Omega(x,y) \\ &\times \sum_{i=1}^{4} R_i(y) - R_5(x)\left(1-\delta_{x,1}\right) + R_5(x+1) \\ &- R_8(x) + R_8(x-1) - \sum_{y=1}^{\infty}\left(R_6(x,y) + R_7(x,y)\right) \\ &+ \frac{1}{2}\sum_{y=1}^{x-1}\left(R_6(x-y,y) + R_7(x-y,y)\right)\left(1-\delta_{x,1}\right)\end{aligned} \tag{11}$$

Benzene:

$$\frac{dB}{dt} = \sum_{x=2}^{\infty}\sum_{i=1}^{5} R_i(x) \tag{12}$$

Styrene:

$$\frac{dS}{dt} = -\sum_{x=1}^{\infty} R_8(x) - R_{10} \tag{13}$$

Catalyst:

$$\frac{dA}{dt} = -R_9 - R_{10} \tag{14}$$

In the above equations, $\Omega(x, y)$ is a function that determines the distribution of scission products; it is given by $1/y$ for random scission.[14] We have neglected the difference in molar mass between benzene and styrene.

As discussed in a previous work,[11] PS contains weak links that undergo scission more easily, and normal links that resist scission better. We showed in that work that the relative number of each kind of link can be calculated as:

$$f_w = \frac{e_w}{e_n + e_w} = \frac{e_w}{\sum_{x=1}^{\infty} xP(x) - \sum_{x=1}^{\infty} P(x)} = 1 - f_n \tag{15}$$

where f_w is the fraction of weak links and f_n is the fraction of normal links.

The time evolution of the concentration of weak links (e_w) can be expressed as:

$$\frac{de_w}{dt} = -\left(k_{S1w}A^2 + k_{S2w}A^2S^2\right)e_w \tag{16}$$

Equation 15 and 16 must be solved together with the mass balances of the species (Equation 11–14). The initial concentration of weak links, $e_w(0)$, is required as input data by the model.

Method of Moments

Since homopolymer molecules may have a degree of polymerization ranging from one to infinity, the resulting set of mass balances is infinite. In order to reduce the size of the system, the method of moments may be applied. This results in a finite set of equations, the solution of which allows calculation of average properties.[12] In order to use the method, it is necessary to apply moment definitions to the mass balance equations. Given a population of PS molecules with a length distribution, and the molar concentration of PS molecules with length x is PS(x), the ath-order moment of the distribution is defined as

$$M_a = \sum_{x=1}^{\infty} x^a \mathrm{PS}(x) \tag{17}$$

Usually the first three moments of the distribution are enough to calculate average properties, such as $\overline{M}_n$ or $\overline{M}_w$. In order to apply the method of moments, the mass balances for the macromolecular species are multiplied by x^a, $a = 0, 1, 2$, and then added up for all allowable values of x. The result is rearranged in terms of moments, so as to obtain a set

of differential equations for the *a*th order moments. Other balance equations may also be rewritten in terms of moments. The resulting equations for the system PS/$AlCl_3$/*S* are:

Benzene:

$$\frac{dB}{dt} = \left[f_w\left(k_{S1w}A^2 + k_{S2w}A^2S^2\right) + f_n\left(k_{S1n}A^4 + k_{S2n}A^4S^1\right) + k_{In}A^2\right]M_1 \quad (18)$$

Styrene:

$$\frac{dS}{dt} = -2k_pA^2S^2M_0 - R_{10} \quad (19)$$

0th-order moment:

$$\frac{dM_0}{dt} = \left[f_w\left(k_{S1w}A^2 + k_{S2w}A^2S^2\right) + f_n\left(k_{S1n}A^4 + k_{S2n}A^4S^1\right)\right](M_1 - 2M_0) - \frac{1}{2}\left(k_{c1}A^2 + k_{c2,1}A^2S^1 + k_{c2,2}A^4S^4\right)M_1^2 \quad (20)$$

1st order moment:

$$\frac{dM_1}{dt} = -\left[f_w\left(k_{S1w}A^2 + k_{S2w}A^2S^2\right) + f_n\left(k_{S1n}A^4 + k_{S2n}A^4S^1\right)\right]M_1 - k_{In}A^2M_1 + 2M_Sk_pA^2S^2M_0 \quad (21)$$

2nd order moment:

$$\frac{dM_2}{dt} = \left[f_w\left(k_{S1w}A^2 + k_{S2w}A^2S^2\right) + f_n\left(k_{S1n}A^4 + k_{S2n}A^4S^1\right)\right]\left(-\frac{M_3}{3} - M_2 + \frac{M_1}{3}\right) + k_{In}A^2(-2M_2 + M_1) + \left(k_{c1}A^2 + k_{c2,1}A^2S^1 + k_{c2,2}A^4S^4\right)M_2^2 + 2k_pA^2S^2(2M_1 + M_0) \quad (22)$$

Fraction of weak links:

$$f_w = \frac{e_w}{M_1 - M_0} = 1 - f_n \quad (23)$$

One should note that in general, when solving for the 2nd PS moment, the 3rd-order moment appears in the equation. In the above equations this was avoided by estimating its value using a closure technique.[15] This technique makes it possible to obtain expressions of the higher order moments in terms of the known lower order ones. In this model we use the expression corresponding to a log-normal distribution (Equation 24).

$$M_3 = M_0\left(\frac{M_2}{M_1}\right)^3 \quad (24)$$

Since the actual shape of the MWD is unknown beforehand, the result is an approximation.

From the moments of the distribution, it is possible to calculate $\overline{M}_n$ and $\overline{M}_w$ as follows:

Number-average molecular weight:

$$\overline{M}_n = 104\frac{M_1}{M_0} \quad (25)$$

Weight-average molecular weight:

$$\overline{M}_w = 104\frac{M_2}{M_1} \quad (26)$$

pgf Transform

The method of moments may be considered a transform technique that changes a very detailed but unsolvable system of infinite equations into a lumped system of finite size that can be solved, producing useful results in terms of the lumped variables. Other transform techniques may be applied for the same purpose, giving other useful results. One of such transform techniques employs pgfs. This method allows calculation of the complete MWD of the treated polymer.[13,16]

The pgf for the length distribution of PS is defined as:

$$\phi_j(z) = \sum_{x=1}^{\infty} p_j(x)z^x \quad j = 0, 1, 2 \quad (27)$$

where *z* is the dummy transform variable, $0 \le |z| \le 1$, $p_j(x)$ is the *j* probability mass function of the length distribution of PS, with *j* taking the values of 0 (numeric), 1 (weight), and 2 (chromatographic). If PS(*x*) represents the molar concentration of the PS molecules of size *x*, then the probability mass fractions are defined as:

$$p_j(x) = \frac{x^j\,\mathrm{PS}(x)}{\sum_{x=1}^{\infty} x^j\,\mathrm{PS}(x)} = \frac{x^j\,\mathrm{PS}(x)}{M_j} \quad x = 1\ldots\infty;\ j = 0, 1, 2 \quad (28)$$

Please note that the resulting expressions are written in terms of the moments M_j ($j = 0,1,2$), defined earlier in the text.

The MWD may be expressed in several forms: number fraction, weight fraction, or differential log distribution, which we will indicate as $n(x)$, $w(x)$ and $dW/d\log_{10} M(x)$. Number and weight probability mass functions are equivalent to $n(x)$ and $w(x)$, respectively. On the other hand, the chromatographic probability mass function $[p_2(x)]$ is related to $dW/d\log_{10} M(x)$ by

$$dW/d\log_{10} M(x) = \frac{1}{\log_{10} e}\frac{p_2(x)M_2}{M_1} \tag{29}$$

In order to transform the mass balances using pgf, every term in Equation (11) is multiplied by $x^a z^x$, $a = 0, 1, 2$, and added up for all possible values of x. The result is reordered in terms of the moments defined in Equation (17) and the pgf defined in Equation (27), yielding a system of differential equations for the different pgf. For our particular system, the differential equations for the three pgf transforms are shown in Equation 30–32.

Number pgf

$$\begin{aligned}\frac{\partial(M_0\phi_0(z))}{\partial t} &= \begin{bmatrix} f_w\left(k_{S1w}A^2 + k_{S2w}A^2S^2\right) \\ +f_n\left(k_{S1n}A^4 + k_{S2n}A^4S^1\right)\end{bmatrix} \\ &\times M_0\left(-z\frac{\partial\phi_0(z)}{\partial z} + 2\frac{\phi_0(z)-z}{z-1}\right) \\ &+ k_{In}A^2(1-z)M_0\frac{\partial\phi_0(z)}{\partial z} \\ &+ \left(k_{c1}A^2 + k_{c2,1}A^2S^1 + k_{c2,2}A^4S^4\right) \\ &\times zM_0\frac{\partial\phi_0(z)}{\partial z}\left(\frac{M_0}{2}z\frac{\partial\phi_0(z)}{\partial z} - M_1\right) \\ &- k_pA^2S^2M_0\phi_0(z)(1-z)\end{aligned} \tag{30}$$

Weight pgf

$$\begin{aligned}\frac{\partial(M_1\phi_1(z))}{dt} &= \begin{bmatrix} f_w\left(k_{S1w}A^2 + k_{S2w}A^2S^2\right) \\ +f_n\left(k_{S1n}A^4 + k_{S2n}A^4S^1\right)\end{bmatrix} \\ &\times\left(-zM_1\frac{\partial\phi_1(z)}{\partial z} + 2\left(M_1\frac{\phi_1(z)}{z-1} + zM_0\frac{1-\phi_0(z)}{(z-1)^2}\right)\right) \\ &+ k_{In}A^2M_1\left((1-z)\frac{\partial\phi_1(z)}{\partial z} - \frac{\phi_1(z)}{z}\right) \\ &+ \left(k_{c1}A^2 + k_{c2,1}A^2S^1 + k_{c2,2}A^4S^4\right) \\ &\times M_1^2\left(z\frac{\partial\phi_1(z)}{\partial z}(\phi_1(z)-1)\right) \\ &+ k_pA^2S^2(M_1\phi_1(z)(z-1) + zM_0\phi_0(z))\end{aligned} \tag{31}$$

Chromatographic pgf

$$\begin{aligned}\frac{\partial(M_2\phi_2(z))}{\partial t} &= \frac{2\begin{bmatrix} f_w\left(k_{S1w}A^2 + k_{S2w}A^2S^2\right) \\ +f_n\left(k_{S1n}A^4 + k_{S2n}A^4S^1\right)\end{bmatrix}}{(z-1)^2} \\ &\times\begin{pmatrix} M_2\phi_2(z)(z-1)^2 + 2M_1\phi_1(z)(z-z^2) \\ +M_0(\phi_1(z)-1)(z+z^2)\end{pmatrix} \\ &-\Big[f_w\left(k_{S1w}A^2 + k_{S2w}A^2S^2\right) \\ &+ f_n\left(k_{S1n}A^4 + k_{S2n}A^4S^1\right)\Big]zM_2\frac{\partial\phi_2(z)}{\partial z} \\ &+ k_{In}A^2\left(M_2\frac{\partial\phi_2(z)}{\partial z}(1-z) + M_1\frac{\phi_1(z)}{z} - 2M_2\frac{\phi_2(z)}{z}\right) \\ &+ \left(k_{c1}A^2 + k_{c2,1}A^2S^1 + k_{c2,2}A^4S^4\right) \\ &\times\left(zM_1M_2\frac{\partial\phi_2(z)}{\partial z}(\phi_1(z)-1) + (M_2\phi_2(z))^2\right) \\ &+ k_pA^2S^2(M_2\phi_2(z)(z-1) + z(2M_1\phi_1(z) + M_0\phi_0(z)))\end{aligned} \tag{32}$$

Equation 30–32 must be solved numerically. The result is the value of each of the three pgf at given values of the dummy variable z. The number, weight and chromatographic probability mass functions, which are related to the MWD as explained before, are recovered through the inversion of the pgf transforms. Since only discrete values of the pgf are available, numerical inversion is the only option. Several methods are available. Each of these methods uses as input the pgf evaluated at a specific set of values z_i, $z_i \in Z$, with Z defined differently in each inversion method. Hence, Equation 30–32 have to be discretized in terms of every $z_i \in Z$ in order to obtain the pgf values needed to recover the MWD from the transform domain.

The inversion method used in this work is an adaptation of the one originally proposed by Papoulis[17] for the inversion of Laplace transforms. Details of the adaptation may be found elsewhere.[13] This particular method was selected because it provides satisfactory results with a computational effort that is modest compared to that required by other inversion methods. The result of the inversion is a discrete set of values of the sought MWD. It has been found previously[13] that the best results are found when recovering each distribution from its own pgf. For example, it is best to recover $n(x)$ from $\phi_0(z)$.

The inversion method recovers the probability mass fractions from their pgf transforms by means of the inversion formula shown in Equation 33,

$$p_j(x) = \mathbf{a}^T\mathbf{l}(e^{-rx}), \quad j = 0, 1, 2 \tag{33}$$

In this equation, $\mathbf{l}(e^{-rx})$ is a vector of dimension $N+1$ whose ith element is a Legendre polynomial of order $2i-2$ evaluated at e^{-rx}, where r is a real number. The Legendre

polynomials can be calculated recursively using the following relationships,[17] where $l^d(s)$ is a Legendre polynomial of order d:

$$\begin{aligned} l^0(s) &= 1 \\ l^1(s) &= s \\ (d+1)l^{d+1}(s) &= (2d+1)sl^d(s) - dl^{d-1}(s) \end{aligned} \tag{34}$$

Additionally, the elements of vector **a** can be calculated by solving the following system of linear equations

$$\mathbf{Aa} = \mathbf{b} \tag{35}$$

where **A** is a lower triangular matrix whose elements are defined as follows:

$$A_{k,m} = \frac{(k-m+1)_{m-1}}{2(k-1/2)_m} \quad m = 1,\ldots,k,\ k = 1,\ldots,N+1$$

with

$$(j)_t = \begin{cases} 1 & t = 0 \\ j(j+1)\ldots(j+t-1) & t > 0 \end{cases} \tag{36}$$

and **b** is a vector of scaled values of the pgf evaluated at equidistant points in a logarithmic scale, as indicated in Equation (37):

$$b_i = r\,p_j(z_i), \quad z_i = \mathrm{e}^{-(2i-1)r} \ , i = 1,\ldots,N+1, \quad j = 0,1,2 \tag{37}$$

Both the scaling of the pgf and the separation between the z_i points are determined by the parameter r.

Both N and r are parameters of the inversion method. Choosing appropriate values for them is essential for a suitable performance of the inversion method. In a previous work[13] we found that good results are obtained by calculating r as a function of x according to Equation (38):

$$r = \ln(2)/x \tag{38}$$

The value of N can be selected as the one that minimizes the sum of squares of the difference between the curves calculated with two successive values of N, according to the criterion proposed by Asteasuain et al.[13] The application of this criterion resulted in the value of $N = 4$ for all cases analyzed in this work. It can be seen from Equation 37 and 38 that the inversion method needs $n_{ev} = 3 \cdot (N+1)$ pgf evaluations for each value of x at which the three probability mass fractions (number, weight, and chromatographic) are computed. Therefore, the value of n_{ev} and the number of points at which the MWD will be recovered determine how many pgf differential equations should be solved.

The mathematical model of the system is composed by the set of equations required to compute the average properties, Equation 14, 16, 18–26, plus the equations needed for the calculation of the MWD, Equation 30–32 discretized in terms of the $z_i \in Z$, Equation 33–38 for the inversion method and Equation 29 for calculating $dW/d\log_{10} M$. This differential-algebraic equations system (DAE) was implemented and solved numerically using a built-in method suitable for stiff systems (DASOLV) available within the commercial software gPROMS (Process Systems Enterprise, Ltd.). This software allows performing simulation activities involving complex mathematical models with a large number of equations and variables. Besides, external routines developed by us in FORTRAN were linked to the gPROMS model for some ancillary calculations related to the initial values of the pgf and the evaluations of the derivatives of the pgf with respect to the dummy variable z. Typical CPU times used in the simulation of MWD averaged 27 s on a desktop PC equipped with Intel Core 2/2.66 GHz/3 GB RAM.

Experimental Section

In order to validate the proposed model, experimental data obtained in our laboratory were used. Commercial PS ($\overline{M}_w$: 271 000 g · mol^{-1}, $\overline{M}_n$: 136 000 g · mol^{-1}) was treated with a wide range of $AlCl_3$ and S concentrations, as shown in Table 2. The

Table 2. Experimental conditions for the PS/$AlCl_3$/*S* reactions.[7]

Parameter	Value
instrument	batch mixer Brabender Plastograph W50
environment	N_2 atmosphere
PS	$\overline{M}_w = 271\,000$, $\overline{M}_n = 136\,000$
reaction time	22 min
temperature	200 °C
sample withdrawal times	intermediate and final times
initial catalyst concentration	0.1, 0.3, 0.5, 0.7, and 1 wt.-% of $AlCl_3$
initial cocatalyst concentration	0.0, 0.3, and 0.6 wt.-% of S

reaction was carried out in a batch mixer (Brabender Plastograph W50) at 200 °C and under nitrogen atmosphere. The mixing procedure was performed at 60 rpm for 22 min. Average molecular weights and MWDs of all samples were obtained by SEC in a Waters Scientific Chromatograph model 150-CV. Average molecular weights obtained for the PS/$AlCl_3$/S experiments were published previously,[7] as well as experimental evidence of the degradation of PS and the compensating effect of S. Reported data correspond to averages of several replications for each data point, ensuring an error level within the instrument accuracy of ±5%. MWDs were not published before. The MWD of the measurement that was closest to the average of the replications of each data point was selected as representative of each set.

Results and Discussion

In order to solve the proposed model and obtain the MWD, the kinetic parameters previously obtained through an optimal fit to experimental average molecular weight data were used.[12] These parameters are shown in Table 3. We used the value of the initial concentration of weak bonds, $e_w(0)$, that was previously determined[11] to be 0.01 mol L^{-1}. The reported parameters allow the model to calculate average molecular weights, producing predictions that agree with experimental data within a 20% error. This was accomplished by using the moments calculated from the corresponding moment equations. Those same moments could in principle be calculated also by algebraic manipulation of the estimated MWD. Although this procedure suffers from significant error propagation, it may provide an indirect proof of the reasonableness of the MWD calculation. With that in mind, we corroborated that the two theoretical predictions of $\overline{M}_w$ for the system $AlCl_3$/PS agreed within 20% for most of the catalyst concentrations. The largest differences in $\overline{M}_w$ estimations were found for the high catalyst concentration of 0.7%, where both the experimental and calculated $\overline{M}_w$ are small, below the detection limit of the SEC instrument used.

Table 3. Kinetic parameters used in the model.[12]

Parameter	Value
k_{S1w}	$2.522 \times 10^{2}\ M^{-2}\ min^{-1}$
k_{S1n}	$7.149 \times 10^{1}\ M^{-4}\ min^{-1}$
k_{In}	$2.000 \times 10^{0}\ M^{-2}\ min^{-1}$
k_{c1}	$1.031 \times 10^{-2}\ M^{-3}\ min^{-1}$
k_i	$1.000 \times 10^{-3}\ min^{-1}$
k_{S2w}	$9.260 \times 10^{6}\ M^{-5}\ min^{-1}$
k_{S2n}	$4.067 \times 10^{4}\ M^{-4}\ min^{-1}$
$k_{c2,1}$	$8.544\ M^{-4}\ min^{-1}$
$k_{c2,2}$	$9.266 \times 10^{8}\ M^{-9}\ min^{-1}$
k_p	$7.158 \times 10^{7}\ M^{-4}\ min^{-1}$
k_d	$1.329 \times 10^{7}\ M^{-4}\ min^{-1}$

For the systems $AlCl_3$/PS and $AlCl_3$/S/PS, we calculated average molecular weights at different reaction times for various $AlCl_3$ concentrations and the corresponding $dW/d\log_{10} M$ at 3 min reaction time. The model captured the complex behavior of $\overline{M}_w$, which depends on the concentrations of both the catalyst ($AlCl_3$) and cocatalyst (S). This may be observed in the examples shown in Figure 1 and 2, where the experimental values are compared with model predictions.

We may observe in Figure 1 that in the absence of S and at the operating conditions used, $\overline{M}_w$ tends to decrease with respect to the initial value. The model successfully predicts

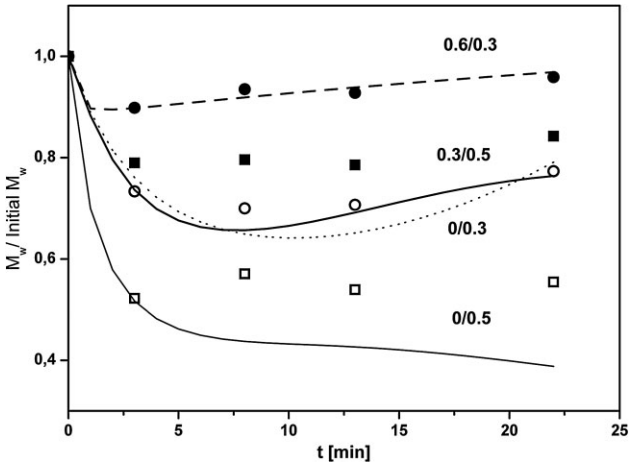

Figure 1. Normalized $\overline{M}_w$ for PS treated with $AlCl_3$ and S in S/A ratios different from unity. Lines: model predictions (– 0.0/0.3; – – 0.6/0.3; — 0/0.5; — 0.3/0.5); symbols: experimental (○ 0.0/0.3; ● 0.6/0.3; □ 0/0.5; ■ 0.3/0.5).

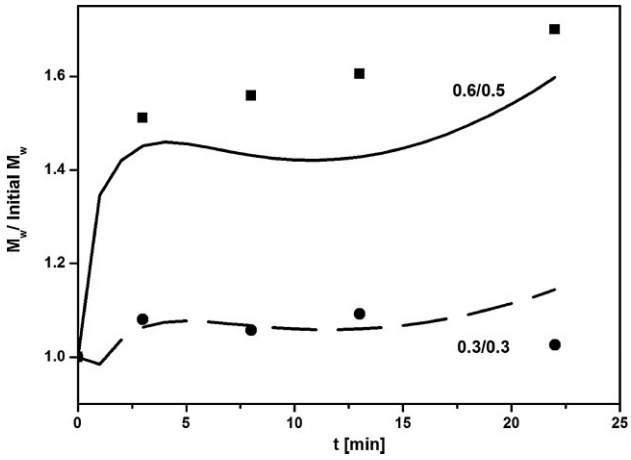

Figure 2. Normalized $\overline{M}_w$ for PS treated with $AlCl_3$ and styrene in S/A ratios close to unity. Lines: model predictions (– – 0.3/0.3; — 0.6/0.5); symbols: experimental (● 0.3/0.3; ■ 0.6/0.5).

that this decrease is sharp during the first few minutes of the reaction. The $\overline{M}_w$ of PS decreases moderately for 0.3% of $AlCl_3$, indicating that cross-linking may be ignored and that chain scission is present. When the content of $AlCl_3$ increases to 0.5%, PS chain scission becomes more evident. For even higher catalyst concentrations, not shown in the figure (1.0–1.5%), it was reported that $\overline{M}_w$ drops dramatically to a tenth of its initial value.[18] Chain scission of PS in the presence of Lewis acids has been attributed to a beta cleavage mechanism.[7–10] This kind of secondary reaction is undesirable for the blend compatibilization at which we aim, since it not only worsens the properties of the blend by reducing the size of the PS blocks, but also competes with the sought copolymerization reaction.[18]

The addition of S counteracts the described behavior to some degree, sometimes even permitting $\overline{M}_w$ to increase. However, if one continues to add *S*, $\overline{M}_w$ tends to decrease again. When the S/A ratios differ from unity, as in the examples in Figure 1, $\overline{M}_w$ tends to decrease. When the S/A ratios approach unity, as in the examples in Figure 2, $\overline{M}_w$ increases. These results suggest that the presence of S may give rise to one o more extra reactions that counteract beta cleavage and compete with it. As discussed in Díaz et al.[7] PS macromolecules are expected to react almost instantaneously with $AlCl_3$. In consequence, S should react with macrocarbocations and unsaturated species formed during scission. It is known that S may polymerize under the influence of heat alone, via a free radical mechanism. As no increment in $\overline{M}_w$ was observed at very low $AlCl_3$ contents for S concentrations of 0.3 and 0.6%, the contribution of free radical polymerization can be discarded at the operating conditions used. Styrene may also react with a macrocarbocation to generate species of higher molecular weight via cationic polymerization. The reaction in Equation 8 is a lumped representation of this reaction. More details on the chemical reactions involved may be found elsewhere.[7] The presence of this reaction could explain the evolution of $\overline{M}_w$ for S/A = 0.3/0.3 and 0.6/0.5 that is shown in Figure 2. Here, the final $\overline{M}_w$ values are up to 60% higher than the one corresponding to the pristine PS. As shown in Díaz et al.,[7] at these S/A ratios the concentrations of macrocarbocations and of S are of the same order of magnitude. This suggests that the S/A ratio may govern the competition between scission and polymerization reactions, and as a result only the addition of an appropriate amount of S is effective in reducing the degradation of PS.

Figure 3 shows the experimental $dW/d\log_{10} M$ of samples that have reacted for 3 min in the presence of different concentrations of $AlCl_3$ only, compared with the theoretical predictions obtained in this work. To ease the analysis, all curves have been normalized so that the maximum height is unity. It may be observed that as the

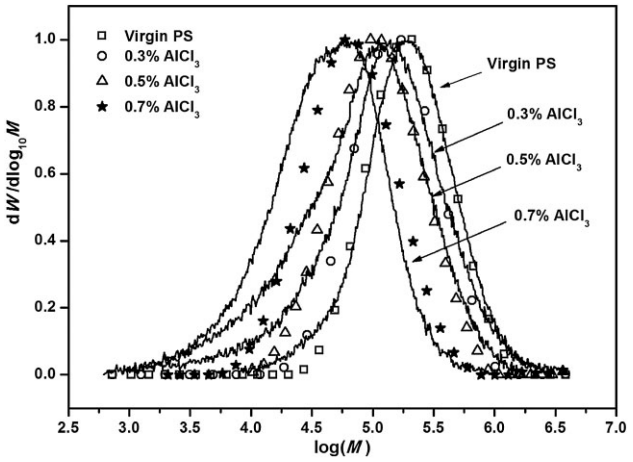

Figure 3. Normalized $dW/d\log_{10} M$ for various [$AlCl_3$] after 3 min of reaction for the system PS/$AlCl_3$. Lines: experimental; symbols: model predictions.

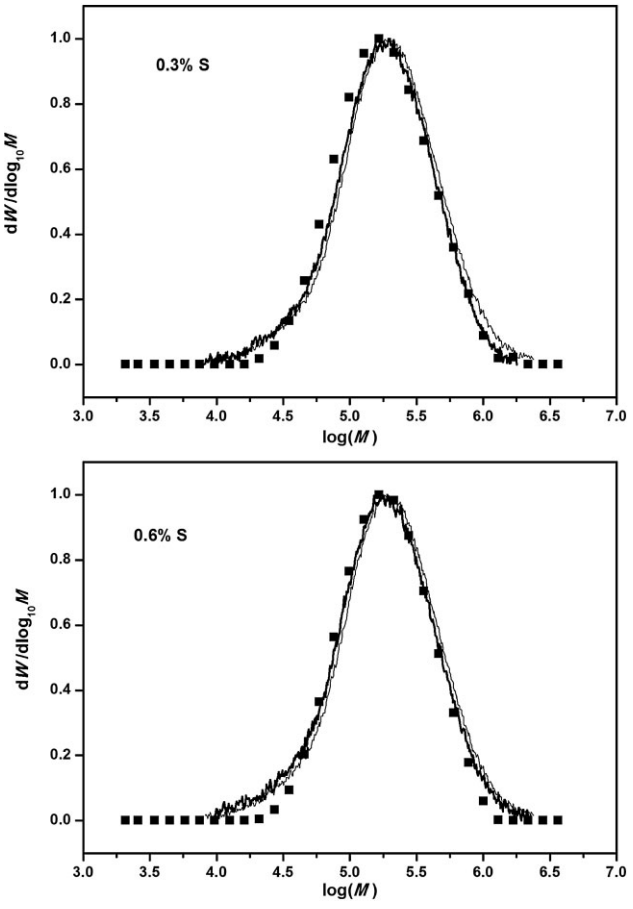

Figure 4. Normalized $dW/d\log_{10} M$ of PS treated with 0.1% of $AlCl_3$ and two levels of styrene at 200 °C and 8 min reaction time. Gray line: experimental virgin resin, black line: experimental modified resin, symbols: simulated modified resin.

concentration of $AlCl_3$ increases, the experimental distribution shifts toward the lower molecular weights. This indicates that at the reaction conditions used PS degrades in the presence of the catalyst. The experimental distributions also widen, showing an increase in polydispersity. This is an indication that the chain combination reactions are not negligible, and that the process cannot be described as a pure scission one. The model predictions agree well with the observed behavior. The calculated curves not only shift toward lower molecular weights but also widen as the concentration of catalyst increases. The agreement with the experimental curves is very good if one considers that the model constants were fitted only to $\overline{M}_w$, and not to the distribution curves. Similar results were obtained for other reaction times.

We also used the proposed model to simulate the MWD for PS treated with 0.1, 0.3, 0.5, 0.7, and 1.0 wt.-% $AlCl_3$ and either 0.3 or 0.6 wt.-% S for reaction times of up to 22 min. As an example, we show in Figure 4–8 the calculated and experimental $dW/d\log_{10} M$ for all the reacting mixtures. All

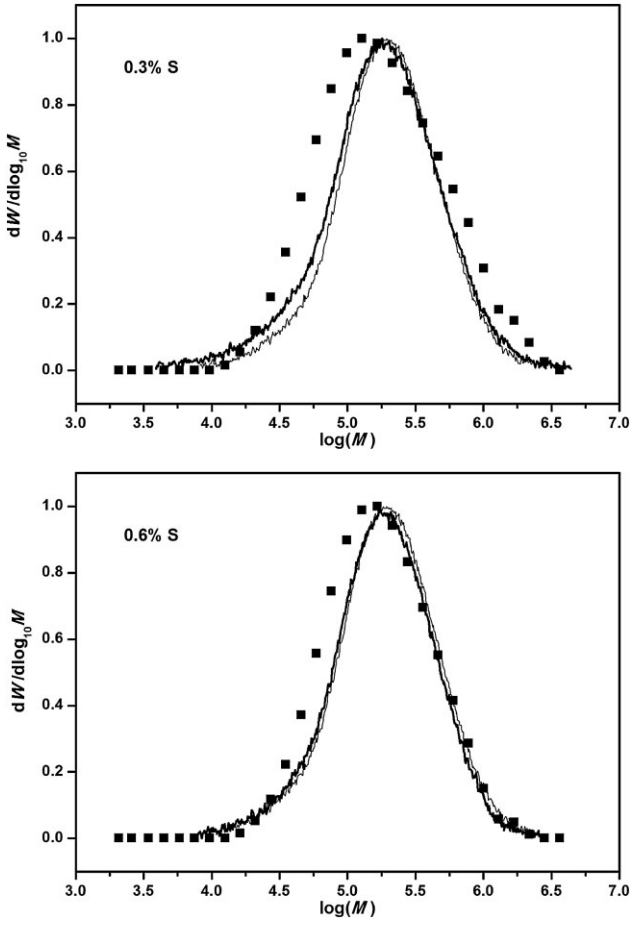

Figure 5. Normalized $dW/d\log_{10} M$ of PS treated with 0.3% of $AlCl_3$ and two levels of styrene. Experimental conditions and symbols as in Figure 4.

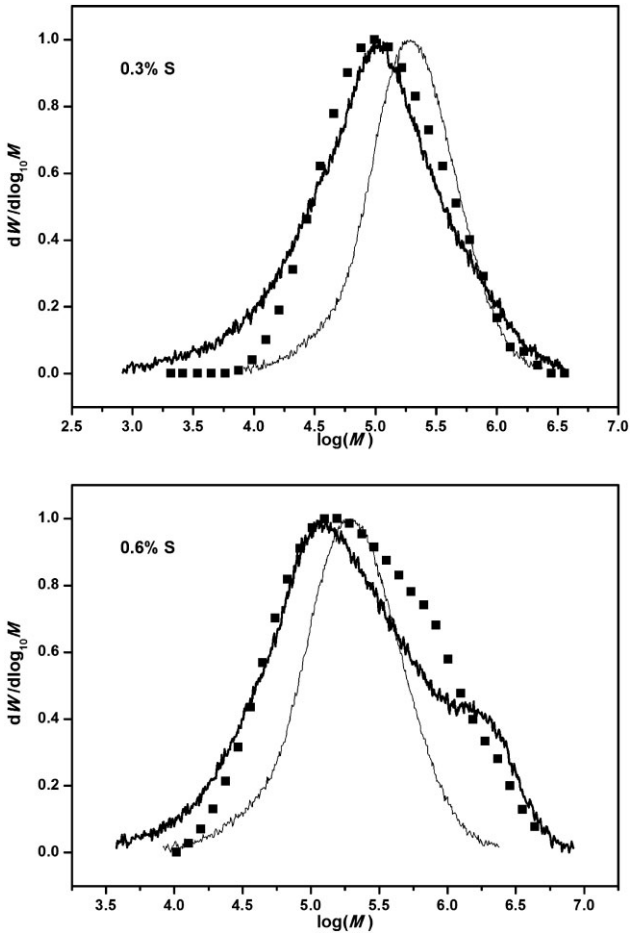

Figure 6. Normalized $dW/d\log_{10} M$ of PS treated with 0.5% of $AlCl_3$ and two levels of styrene. Experimental conditions and symbols as in Figure 4.

results are shown at 8 min of reaction except in the case of Figure 7 (a). For that figure, the molecular weight at 8 min dropped below the detection limit of the instrument, so results at 5 min are shown instead. No experimental values above the instrument detection limit are available for the conditions of Figure 8 (a) at any reaction time, so only the estimated $dW/d\log_{10} M$ is shown. In all the figures the $dW/d\log_{10} M$ of the pristine polymer is also shown for comparison. Model predictions agree well with the experimental data, although some deviations occur, in particular in the low-molecular-weight region.

Figure 4 and 5 correspond to cases where the catalyst concentration is very low, producing only a slight modification of the pristine PS. It may be observed that the model predicts correctly the minimal degree of change produced under these conditions. In the absence of S the modification is larger at the same $AlCl_3$ concentrations. For example, the curve corresponding to 0.3% of $AlCl_3$

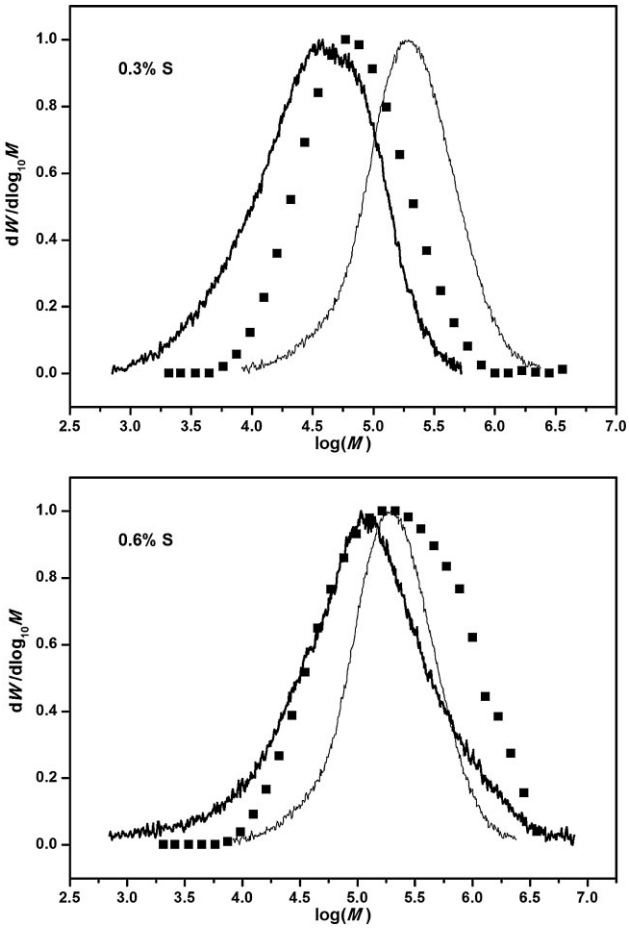

Figure 7. Normalized dW/d $\log_{10}$ M of PS treated with 0.7% of $AlCl_3$ and two levels of styrene at 200 °C. (a) At 5 min of reaction and 0.3% S; (b) at 8 min of reaction and 0.6% S. Symbols as in Figure 4.

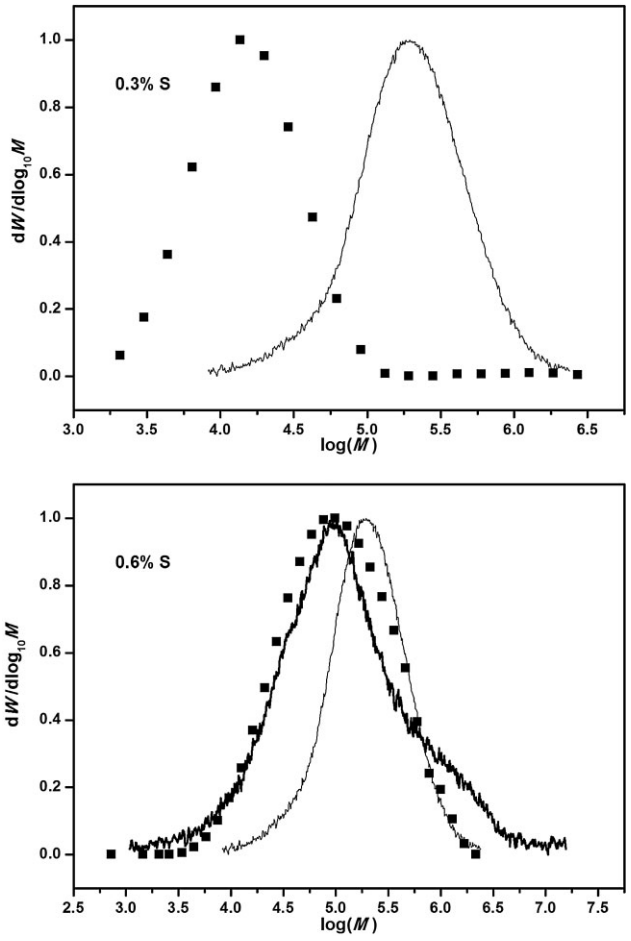

Figure 8. Normalized dW/d $\log_{10}$ M of PS treated with 1.0% of $AlCl_3$ and two levels of styrene. Experimental conditions and symbols as in Figure 4.

in Figure 3 departs significantly from the one corresponding to the virgin resin. By contrast, the curves corresponding to modified and virgin resin in Figure 5 are very close. This is an indication of the compensating effect of the addition of the cocatalyst to the system.

In the case of Figure 6, corresponding to a catalyst concentration of 0.5 wt.-%, the model is able to predict correctly both the widening of the distribution and the shift of the peak for both concentrations of cocatalyst. It can be seen that for a 0.6 wt.-% S the model can predict qualitatively the increase in the fraction of high molecular weight molecules, even if the calculated $\overline{M}_w$ for that particular time is not exact (see Figure 2).

In Figure 7 we show the results of dW/d $\log_{10}$ M for material treated with 0.7 wt.-% of catalyst and two concentrations of S. It may be observed that for 0.3 wt.-% S the model predicts a shift of the MWD in the direction of the low-molecular-weights, although the shift is smaller than the one experimentally found. For 0.6 wt.-% S, calculated and experimental shifts coincide and are less pronounced than for 0.3 wt.-% S. This smaller shift agrees with the effect of the ratio S/A on $\overline{M}_w$ shown in Figure 1 and 2 for other catalyst concentrations. Finally, the results for PS treated with 1 wt.-% $AlCl_3$ are shown in Figure 8. It can be seen that for 0.3 wt.-% S the calculated MWD shows an important shift in the direction of the lower molecular weights, indicating a large decrease in the molecular weight. This agrees with the experimental results, although for the reasons already discussed the experimental curve is not available. For S concentrations of 0.6 wt.-%, as in the previous cases, the model predicts adequately the change suffered by the MWD, but a deviation is observed in the high molecular weight region, where concentrations are underestimated. This agrees with the underestimation of average molecular weights at this time reported elsewhere.[12]

Conclusion

We propose a model for the catalytic degradation of PS in presence of $AlCl_3$/*S* that may calculate both average molecular weights and complete MWD through the application of the moment and the pgf techniques. The model was validated experimentally, showing that its predictions are in agreement with experimental data. Although it is relatively simple, the model is successful in reproducing a very complex behavior. In the presence of S it is necessary to account not only for the competing effects of the scission and combination reactions but also for the S polymerization reactions in order to explain the changes observed in the MWD. According to the observed results, the ratio *S/A* is the variable to be manipulated in order to control degradation during processing at the studied temperature. If the objective is to use Friedel-Crafts alkylations for compatibilization purposes, the mass ratio of $AlCl_3$ to S should be kept close to unity to minimize degradation of PS. In a graft copolymerization setting, this would be important to minimize the competition between the grafting and degradation reactions, improving the compatibilizing capacity of the copolymer.

Acknowledgements: The authors are grateful for the financial support from CONICET (National Research Council of Argentina), ANPCyT (National Agency for Promotion of Science and Technology of Argentina), and UNS (Universidad Nacional del Sur).

Received: January 4, 2011; Published online: April 12, 2011; DOI: 10.1002/mren.201100001

Keywords: degradation; modeling; molecular weight distribution/molar mass distribution; polystyrene (PS)

[1] Y. J. Sun, W. E. Baker, *J. Appl. Polym. Sci.* **1997**, *65*, 1385.
[2] Y. J. Sun, R. J. G. Willemse, T. M. Liu, W. E. Baker, *Polymer* **1998**, *39*, 2201.
[3] M. F. Díaz, S. E. Barbosa, N. J. Capiati, *Polymer* **2002**, *43*, 4851.
[4] M. F. Díaz, S. E. Barbosa, N. J. Capiati, *Polymer* **2007**, *48*, 1058.
[5] Y. Gao, H. Huang, Z. Yao, D. Shi, Z. Ke, J. Yin, *J. Polym. Sci., Part B: Polym. Phys.* **2003**, *41*, 1837.
[6] Z. Guo, Z. Fang, L. Tong, Z. Xu, *Polym. Degrad. Stab.* **2007**, *92*, 545.
[7] M. F. Díaz, S. E. Barbosa, N. J. Capiati, *J. Appl. Polym. Sci.* **2009**, *114*, 3081.
[8] B. Pukánszky, J. P. Kennedy, T. Kelen, F. Tüdõs, *Polym. Bull.* **1981**, *5*, 469.
[9] V. Karmore, G. Madras, *Ind. Eng. Chem. Res.* **2002**, *41*, 657.
[10] H. Nanbu, Y. Sakuma, Y. Ishihara, T. Takesue, T. Ikemura, *Polym. Degrad. Stab.* **1987**, *19*, 61.
[11] I. A. Gianoglio Pantano, M. F. Díaz, A. Brandolin, C. Sarmoria, *Polym. Degrad. Stab.* **2009**, *94*, 566.
[12] I. A. Gianoglio Pantano, A. Brandolin, C. Sarmoria, *Polym. Degrad. Stab.* **2011**, *96*, 416.
[13] M. Asteasuain, A. Brandolin, C. Sarmoria, *Polymer* **2002**, *43*, 2529.
[14] B. J. McCoy, M. Wang, *Chem. Eng. Sci.* **1994**, *49*, 3773.
[15] R. C. M. Zabisky, W.-M. Chan, P. E. Gloor, A. E. Hamielec, *Polymer* **1992**, *33*, 2243.
[16] M. Asteasuain, C. Sarmoria, A. Brandolin, *Polymer* **2002**, *43*, 2513.
[17] A. Papoulis, *Q. Appl. Math.* **1956**, *14*, 405.
[18] S. Barbosa, M. Díaz, G. Mabe, E. A. Brignole, N. J. Capiati, *J. Polym. Sci., Part B: Polym. Phys.* **2005**, *43*, 2361.